

The Multiple Chemokine–Binding Bovine Herpesvirus 1 Glycoprotein G (BHV1gG) Inhibits Polymorphonuclear Cell but Not Monocyte Migration into Inflammatory Sites

Zheng Liu,¹ Ramalingam Bethunaickan,¹ Ranjit Sahu,¹ Max Brenner,² Teresina Laragione,² Percio S Gulko² and Anne Davidson¹

¹Center for Autoimmune and Musculoskeletal Diseases and ²Center for Genomics and Human Genetics, The Feinstein Institute for Medical Research, Manhasset, New York, United States of America

Chemokines facilitate the recruitment of inflammatory cells into tissues, contributing to target organ injury in a wide range of inflammatory and autoimmune diseases. Targeting either single chemokines or chemokine receptors alters the progression of disease in animal models of rheumatoid arthritis and lupus with varying degrees of efficacy, but clinical trials in humans have been less successful. Given the redundancy of chemokine–chemokine receptor interactions, targeting of more than one chemokine may be required to inhibit active inflammatory disease. To test the effects of multiple chemokine blockade in inflammation, we generated an adenovirus expressing bovine herpesvirus 1 glycoprotein G (BHV1gG), a viral chemokine antagonist that binds to a wide spectrum of murine and human chemokines, fused to the fragment crystallizable (Fc) portion of murine immunoglobulin (IgG)2a. Administration of the adenovirus significantly inhibited thioglycollate-induced migration of polymorphonuclear leukocytes into the peritoneal cavity of BALB/c mice and reduced both clinical severity and articular damage in K/BxN serum transfer-induced arthritis. However, treatment with BHV1gG-Ig fusion protein did not prevent monocyte infiltration into the peritoneum in the thioglycollate model and did not prevent renal monocyte infiltration or nephritis in lupus-prone NZB/W mice. These observations suggest that the simultaneous inhibition of multiple chemokines by BHV1gG has the potential to interfere with acute inflammatory responses mediated by polymorphonuclear leukocytes, but is less effective in chronic inflammatory disease mediated by macrophages.

Online address: <http://www.molmed.org>

doi: 10.2119/molmed.2012.00339

INTRODUCTION

Autoimmune disease occurs when the immune system loses tolerance toward self-antigens and the resulting immune response causes tissue damage. Systemic autoimmune diseases such as rheumatoid arthritis (RA) and systemic lupus erythematosus (SLE) are characterized by the production of autoantibodies to ubiquitously expressed antigens as well as local inflammation in peripheral tissues.

Leukocyte infiltration is found commonly in the inflamed organs and contributes to the eventual tissue damage.

Chemokines, which are essential in directing leukocyte trafficking, have been associated with the pathogenesis of RA and lupus nephritis. Synovial tissue and synovial fluids of RA patients contain higher levels of CXCL9, CXCL10, CXCL11, CXCL12, CCL2, CCL3, CCL13, CCL18, CCL21 and

CXC3CL1 compared with healthy individuals (1). CCR2 deficiency is protective in the K/BxN serum transfer model (2), and antagonists of CXCR3 (3) and CXCL13 (4) reduce disease severity and joint damage in murine arthritis. However, while anti-CXCL10 antibodies achieved a significant, albeit modest, benefit (5) in RA patients, antagonists of CCR2 and CCR5 failed to show clinical efficacy (6–8). In a similar fashion, studies in lupus-prone NZB/W F1 mice have shown upregulation of chemokines including CXCL13, CCL2, CCL3, CCL9 and CCL20 in the kidneys following initial immune complex deposition, with subsequent recruitment of many other chemokines as the disease progresses. This is associated with the progressive renal accumulation of macrophages and dendritic cells as well as activated CD4 T cells and B cells (9).

Address correspondence to Anne Davidson, Feinstein Institute for Medical Research, 350 Community Drive, Manhasset NY 11030. Phone: 516 562 3840; Fax: 516 562 2953; E-mail: adavidson1@nshs.edu.

Submitted November 29, 2012; Accepted for publication August 21, 2013; Epub (www.molmed.org) ahead of print August 21, 2013.

The Feinstein Institute
for Medical Research 

Deficiency of *CCL2*, *CCR2* or *CXCR3* reduces renal inflammation and protects the renal function of lupus-prone MRL/lpr mice (10–12), but, not surprisingly, chemokine antagonists have a more modest effect when used later in disease (13–14). These studies, in sum, suggest that it might be necessary to simultaneously inhibit multiple chemokines to more effectively inhibit inflammatory processes and tissue damage in autoimmune diseases.

In this study, we generated an adenovirus expressing a fusion protein containing the secreted form of bovine herpesvirus 1 glycoprotein G (BHV1gG) and the CH2-CH3 portion of murine IgG2a. BHV1gG is a glycoprotein that is expressed on the surface of BHV1-infected cells and is secreted after proteolytic cleavage (15). BHV1gG binds to a wide range of human and murine chemokines (15), some of which, including *CCL2*, *CCL3*, *CCL5*, *CXCL1*, *CXCL12* and *CXCL13* are increased in RA or lupus nephritis. We show here that BHV1gG-Ig greatly reduced thioglycollate-induced neutrophil and eosinophil migration into the peritoneal cavity of BALB/c mice. BHV1gG-Ig also significantly reduced disease severity and joint damage of K/BxN serum-induced arthritis. However, repeated administration of BHV1gG-Ig did not prevent thioglycollate-induced macrophage migration into the peritoneal cavity of BALB/c mice or alter the course of lupus nephritis in NZB/W F1 mice.

MATERIALS AND METHODS

Generation of an Adenovirus Expressing BHV1gG-Ig (Ad-BHV1gG-Ig)

cDNA encoding the secreted form of BHV1gG (kindly provided by Antonio Alcamí) was fused to a $\beta 2$ microglobulin signal sequence as described previously (16) and to the CH2-CH3 domains of murine IgG2a lacking Ig receptor binding capability (17) using a linker sequence (5' GGT GGT GGT TCT GGT GGT GGT TCT GAC TAC AAG GAC GAC GAT GAC AAG GGA GGA

GGA TCT GGA GGA GGT AGC 3') containing a FLAG tag. The construct was expressed in Adeno-X adenovirus according to the manufacturer's directions (BD Clontech, Palo Alto, CA, USA). Serum from a severe combined immunodeficiency (SCID) mouse injected 4 d previously with 1×10^{11} viral particles of Ad-BHV1gG-Ig was applied to a Protein A column and the fusion protein eluted with 0.1 mol/L acetic acid pH 4. The purified protein was then run on a 7.5% SDS gel and a Western blot performed using biotin-conjugated goat anti-mouse IgG2a (1:1000) (Southern Biotechnology Association, Birmingham, AL, USA) as the probing antibody, followed by IRDye 680LT streptavidin (1:5000) (LI-COR Biosciences, Lincoln, NE, USA). The blot was visualized using an Odyssey Imaging System (LI-COR Biosciences).

Measurement of Serum BHV1gG-Ig Concentration

Serum BHV1gG-Ig levels in SCID mice injected 4 d previously with 1×10^{11} viral particles of Ad-BHV1gG-Ig were measured as described previously (17) using a murine IgG2a-specific enzyme-linked immunosorbent assay (ELISA). Standard curves were established using serial dilutions of a control fusion protein. SCID serum contained >10 mg/mL of BHV1gG-Ig protein and was used for all *in vitro* experiments. SCID serum containing a comparable concentration of a control fusion protein, B cell activating factor receptor Ig (BAFF-R-Ig), was used in control experiments.

To measure serum BHV1gG-Ig levels in BALB/c mice, ELISA plates (Falcon Labware, Lincoln Park, NJ, USA) were coated with mouse anti-FLAG monoclonal antibody (Sigma-Aldrich, St. Louis, MO, USA), blocked and incubated sequentially with sera from Ad-BHV1gG-Ig injected BALB/c mice, followed by horseradish peroxidase (HRP)-conjugated goat anti-mouse IgG2a (1/4000 in PBS/1%BSA) (Southern Biotechnology Association) and peroxidase substrate solution (KPL, Gaithers-

burg, MD, USA). Standard curves were established using serial dilutions of sera from Ad-BHV1gG-Ig-treated SCID mice whose BHV1gG-Ig concentration was predetermined as described above.

To determine the half-life of BHV1gG-Ig, five BALB/c mice were injected with SCID serum containing 500 μ g BHV1gG-Ig, and serum BHV1gG-Ig concentrations were measured at intervals and plotted over time. The half-life of BHV1gG-Ig is approximately 7 d (data not shown).

Calcium Flux Assay

Ten million peritoneal cells from NZW mice containing 80% B cells were loaded with 5 μ g/mL of Indo-1 AM (Invitrogen, Carlsbad, CA, USA) at 37°C for 1 h and then stimulated with recombinant murine CXCL13 (0.2 μ g/mL) (R&D Systems, Minneapolis, MN, USA) together with increasing concentrations of BHV1gG-Ig (2 μ g/mL, 8 μ g/mL or 16 μ g/mL), providing a molar ratio (BHV1gG-Ig:CXCL13) of 1.4, 5.7 or 11.4, respectively. BAFF-R-Ig at similar molar ratios and control SCID serum were used as controls. The ratio of fluorescence at 400 nmol/L versus 510 nmol/L was measured by flow cytometry (BD Biosciences, San Diego, CA, USA). Results represent four independent experiments.

Transwell Chemotaxis Assays

One μ g/mL of recombinant murine CXCL13 (R&D Systems) was preincubated with 40 μ g/mL of BHV1gG-Ig (molar ratio BHV1gG-Ig:CXCL13 = 5.7) or BAFF-R-Ig in migration medium (0.5% BSA [Sigma-Aldrich], 20 mmol/L HEPES [Cellgro, Mediatech, Herndon, VA, USA], RPMI-1640 medium [Sigma-Aldrich]) at 37°C for 30 min in the lower chambers of a fibronectin-coated transwell plate (5.0 μ mol/L pores, Costar, Corning, NY, USA). One million peritoneal cells from NZB/W mice containing CXCR5-expressing B1 cells were added to the upper chamber of the transwell inserts. Cells in the lower chambers were collected after 3 h of incubation at 37°C. Cells were then stained with anti-B220 PE, anti-CD4 FITC and anti-CD11b

FITC antibodies (BD Biosciences), and analyzed using flow cytometry (BD Biosciences). The number of B cells that spontaneously migrated to the lower chamber containing only migration medium was consistently below 1% of the input cells.

BM Neutrophils from BALB/c mice, identified as Gr1^{hi}CD11b^{hi}, were isolated by FACS sorting. An *in vitro* migration assay of neutrophils was performed as described previously (18). Briefly, 100 ng/mL of recombinant mouse CXCL1 (R&D Systems) was preincubated with 0, 0.25 or 1, 4 µg/mL of BHV1gG-Ig or 4 µg/mL of BAFF-R-Ig as control in the lower chambers of a transwell plate (5.0 µmol/L pores, Costar). 2×10^5 BM neutrophils were added to the upper chambers. Cells in the lower chambers were collected after 1 h of incubation at 37°C. Cells were stained with anti-F480 PE, anti-Gr1 APC and anti-CD11b FITC antibodies (BD Biosciences), and analyzed using flow cytometry (BD Biosciences).

An *in vitro* migration of macrophages was performed as described previously (19). Briefly, 10 ng/mL of recombinant mouse CCL2 (R&D Systems) was preincubated with 0, 25, 100 or 400 ng/mL of BHV1gG-Ig or 400 ng/mL of BAFF-R-Ig as control in the lower chambers of a transwell plate (8.0 µmol/L pores) (Costar). Two hundred thousand mouse peritoneal cells that were harvested 72 h after an intraperitoneal (IP) injection of 1 mL of 4% thioglycollate into BALB/c mice were added to the upper chambers. After 4 h of incubation at 37°C, transwell filters were fixed in methanol and stained with May-Grunwald-Giemsa. The cells that attached to the filter were counted by light microscopy.

Thioglycollate-Induced Peritonitis

Groups of 5 BALB/c mice were injected intravenously (IV) with Ad-BHV1gG-Ig (1×10^{11} viral particles/mouse) or a similar dose of control adenovirus expressing BAFF-R-Ig or β-galactosidase (Ad-LacZ) or no treatment. Four days later, the mice

were injected IP with 1 mL of 4% sterile thioglycollate (BD Diagnostic Systems, Franklin Lakes, NJ, USA). The mice were euthanized 4 h or 72 h later and peritoneal cells were harvested and analyzed using flow cytometry (20). Similar experiments were performed 12 h after intraperitoneal delivery of four-fold increasing doses of BHV1gG protein up to 1 mg.

Detection of Anti-BHV1gG-Ig Antibody

ELISA plates (Falcon Labware) were coated with 0.5 µg/mL of BHV1gG-Ig, blocked and incubated sequentially with dilutions of sera from Ad-BHV1gG-Ig-treated or control NZB/W F1 mice followed by HRP-conjugated goat anti-mouse IgG1, 2b and 3 (1/4000 in PBS/1% BSA) (Southern Biotechnology Association) and peroxidase substrate solution (KPL). ELISA data was normalized to a high-titer serum assigned an arbitrary level of 512U and run in serial dilution on each plate.

Ad-BHV1gG-Ig Treatment of Mice with K/BxN-Induced Arthritis

Ten week-old BALB/c mice were injected with Ad-BHV1gG-Ig or Ad-LacZ on d -4, and 200 µL of K/BxN (KRN) serum was administered IP at d 0 and d 2. The clinical arthritis severity (clinical score) of each paw was determined based on a 0 to 12 score per mouse per day (21) by an observer blinded to the treatment group (PG). Area under curve (Auc) was used to assess disease severity over the entire course of the experiment and was calculated as the sums of the scores for each individual mouse during the test period. Ankle diameter was measured with a digital caliper. In separate experiments, mice were euthanized 5 d after the induction and mRNA extracted from whole ankle was used for analysis of cytokines and matrix metalloproteases (MMPs) using quantitative real-time PCR (qPCR) as described previously (9, 22) using the following primers: TNFα 5'-TGG GAG TAG ACA AGG TAC AAC CC, CAT CTT CTC

AAA ATT CGA GTG ACA A; IL-1β 5'-TGT AAT GAA AGA CGG CAC ACC, 3'-TCT TCT TTG GGT ATT GCT TGG; MMP-2 5'-TAA CCT GGA TGC CGT CGT, 3'-TTC AGG TAA TAA GCA CCC TTG AA; MMP-3 5'-TTG TTC TTT GAT GCA GTC AGC, 3'-GAT TTG CGC CAA TGC; IL-6 primer mix (Catalog number: PPM03015A – 200) (Superarray, Frederick, MD, USA)

BHV1gG-Ig Treatment of NZB/W Mice

Groups of five to eight 24-wk-old NZB/W mice were injected IP with 500 µg BHV1gG-Ig or control IgG three times a week for 10 wks or received no treatment. The mice were bled every other week and monitored for proteinuria weekly. A subgroup of BHV1gG-Ig-treated mice with established proteinuria was euthanized and kidney sections were analyzed microscopically using hematoxylin and eosin (H & E) staining. In an alternative experiment, NZB/W mice were injected IV with an adenovirus expressing IFNα (3.3×10^9 viral particles) at 12 wks of age to induce disease within a 6- to 8-wk period as described previously (22). A group of 10 mice was injected IP with 500 µg BHV1gG-Ig three times a week from wk 13 to wk 21. Another group of seven mice received the same regimen from wk 15 until the end of the experiment. Control mice were left untreated.

Statistics

Survival data were analyzed using Kaplan-Meier curves and log-rank test. Other comparisons were performed using Mann-Whitney test. *P* values ≤ 0.05 were considered significant.

RESULTS

Generation of the BHV1gG-Ig Protein

The BHV1gG-Ig fusion protein with a predicted molecular weight of 66 kD was produced in the serum of SCID mice as a monomer (Figure 1B). The protein was expressed at a high concentration in the serum of Ad-BHV1gG-Ig injected SCID mice (average of 20 mg/mL).

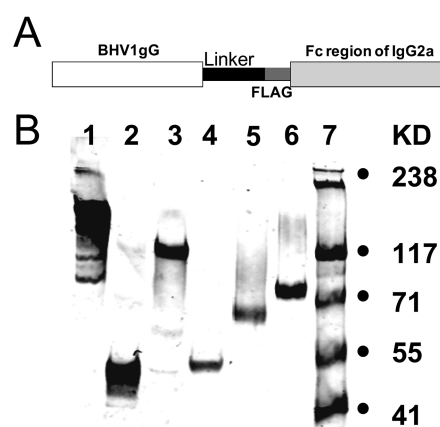


Figure 1. Generation of BHV1gG-Ig protein. (A) A map of the construct of BHV1gG-Ig fusion protein. (B) Western blot analysis of recombinant mouse IgG2a (lane 1 and 2), purified CTLA4-Ig (lane 3 and 4) and purified BHV1gG-Ig (lane 5 and 6) under non-reducing (lane 1, 3 and 5) and reducing (lane 2, 4 and 6) conditions.

BHV1gG-Ig Inhibits Chemokine-Induced *In Vitro* Cell Migration and Calcium Flux

BHV1gG binds a wide range of chemokines *in vitro* (15). To determine whether the BHV1gG-Ig fusion protein is functional, we determined whether it inhibits signaling and cell migration induced by CXCL13, a chemokine that is upregulated in the early stage of nephritis in NZB/W F1 mice (9) and in synovial tissues from RA patients and arthritic mice (23–24). Treatment with 0.2 $\mu\text{g}/\text{mL}$ of recombinant CXCL13 induced a calcium flux in peritoneal B220⁺ cells from NZW mice that express the CXCL13 receptor CXCR5 (Figures 2A–C). Preincubation of CXCL13 with 8 $\mu\text{g}/\text{mL}$ (molar ratio = 5.7) or 16 $\mu\text{g}/\text{mL}$ (molar ratio = 11.4) of BHV1gG-Ig completely inhibited this calcium flux, whereas preincubation with BAFF-R-Ig or control SCID serum had no effect (see Figures 2B, C). A lower concentration of BHV1gG-Ig (2 $\mu\text{g}/\text{mL}$) failed to inhibit CXCL13-induced calcium flux (see Figure 2A). We therefore used a 5.7 molar excess (40-fold excess with respect to concentration) for subsequent experiments. 40 $\mu\text{g}/\text{mL}$ of BHV1gG-Ig inhib-

ited CXCL13-induced (1 $\mu\text{g}/\text{mL}$) migration of the cells in a transwell system. The addition of CXCL13 together with control BAFF-R-Ig resulted in migration of approximately 60% of the input B cells (Figure 2D). In contrast, less than 20% of the input B cells migrated toward CXCL13 preincubated with BHV1gG-Ig (see Figure 2D), demonstrating a significant inhibition of cell migration ($P = 0.0265$). Spontaneous migration was consistently less than 1% of input cells (data not shown).

Similarly, a 5.7 mol/L excess of BHV1gG-Ig:chemokine significantly inhibited the *in vitro* migration of mouse BM neutrophils toward CXCL1 (Figure 2E; $p = 0.0265$, BVH1gG-Ig 4 $\mu\text{g}/\text{mL}$ versus BAFF-R-Ig 4 $\mu\text{g}/\text{mL}$). This inhibition shows a trend toward dose dependency (see Figure 2E). In contrast, a 5.7 mol/L BHV1gG-Ig excess did not prevent the *in vitro* migration of mouse peritoneal macrophages toward CCL2 (Figure 2F).

Ad-BHV1gG-Ig Treatment Significantly Inhibits Thioglycollate-Induced Neutrophil Migration in BALB/c Mice

We next determined whether BHV1gG-Ig inhibits chemokine-induced cell migration *in vivo*. Sterile peritonitis was induced by IP injection of thioglycollate in BALB/c mice that were injected previously with Ad-BHV1gG-Ig, with an adenovirus expressing the control fusion protein BAFF-R-Ig (Ad-BAFF-R-Ig), with a control virus (Ad-LacZ) or with no treatment. Thioglycollate injection led to a rapid increase in the number and percentage of Gr1^{hi} peritoneal neutrophils in the mice receiving the control Ad-LacZ adenovirus or no treatment and this increase was inhibited significantly by Ad-BHV1gG-Ig but not by Ad-BAFF-R-Ig at 4 h (Figure 3C). An increase in the percentage and number of eosinophils and small macrophages was observed in the peritoneal cavity of Ad-LacZ-treated mice 72 h after thioglycollate injection, but only the eosinophilia was inhibited by the treatment of Ad-BHV1gG-Ig (Figure 3D). The serum concentration of BHV1gG-Ig in the Ad-BHV1gG-Ig-

treated mice was $3.4 \pm 2.7 \text{ mg}/\text{mL}$ 4 h after thioglycollate injection and declined to $1.9 \pm 1.3 \text{ mg}/\text{mL}$ 72 h later. When we used BHV1gG protein given IP we reliably detected a >50% decrease in neutrophil migration into the peritoneum only when serum BHV1gG concentrations were >200 $\mu\text{g}/\text{mL}$ (not shown), confirming that an excess of BHV1gG is needed to inhibit chemokine activity *in vivo*.

Ad-BHV1gG-Ig Treatment Reduces the Severity of K/BxN Serum-Induced Arthritis in BALB/c Mice

The K/BxN serum transfer model has acute onset and is highly dependent on infiltrating neutrophils (25). Therefore, we next tested whether Ad-BHV1gG-Ig treatment could alter the outcome of K/BxN serum-induced arthritis. The severity of the disease was evaluated based on the degree of joint inflammation (clinical score) and swelling of the ankles (diameter). As expected, high clinical scores were observed in Ad-LacZ-treated controls 9 d after the first K/BxN serum injection; joint inflammation then diminished during the rest of the experiment (Figures 4A, C). A second experiment confirmed this result and was terminated at d 10 when disease resolved in the BHV1gG-treated mice (Figures 4B, D). Ad-BHV1gG-Ig-treated mice showed significantly lower clinical scores than the controls at multiple times (see Figures 4A, B). In accordance with the clinical scores, ankle swelling was attenuated significantly by the treatment of Ad-BHV1gG-Ig (see Figures 4C, D). The overall severity of disease throughout the entire course of the experiment was also lower in Ad-BHV1gG-Ig-treated mice compared with Ad-LacZ-treated controls (Figure 4). Histological study of joints from mice harvested at d 27 revealed synovial hyperplasia and cartilage erosion in three of five of the arthritis mice receiving the Ad-LacZ control. In contrast, only one of five mice in the Ad-BHV1gG-Ig-treated group showed any of these histologic features (Figures 4E, F). Analysis of the joints from mice har-

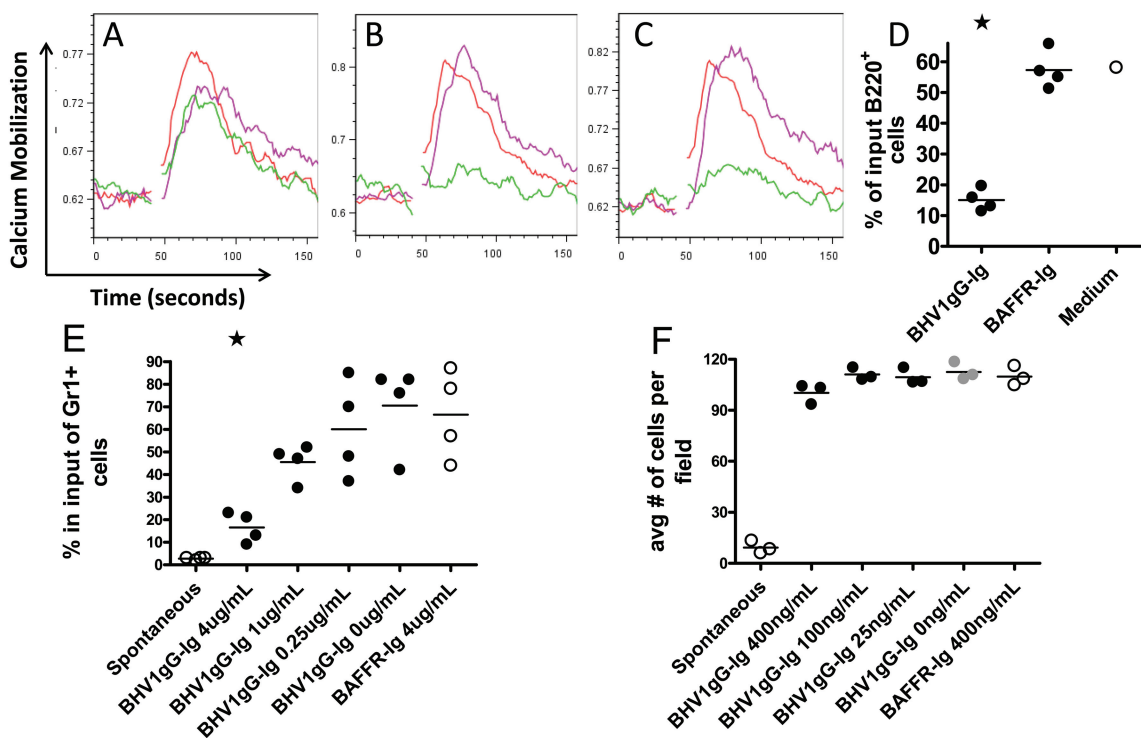


Figure 2. BHV1gG-Ig inhibits CXCL13 and CXCL1 but not CCL2 function *in vitro*. 0.2 µg/mL of recombinant CXCL13 together with 2 µg/mL (A), 8 µg/mL (B) or 16 µg/mL (C) of BHV1gG-Ig (black) was added to peritoneal cells from NZW mice. For control experiments, BAFF-R-Ig (dark gray) at the same concentration or control SCID serum (light gray) was used. Calcium flux was measured using flow cytometry. Data is representative of four experiments. (D) Mouse peritoneal cells (1×10^6) were placed in each of the upper chambers of a transwell. Medium containing 1 µg/mL recombinant mouse CXCL13 together with 40 µg/mL of BHV1gG-Ig ($n = 4$), 40 µg/mL of BAFF-R-Ig ($n = 4$) or medium alone ($n = 1$) was placed in the lower chambers. Data represent the percentage of B220⁺ cells in the lower chamber divided by the total input of B220⁺ cells after 3 h of incubation at 37°C. (E) Sorted mouse BM neutrophils (2×10^5) were placed in each of the upper chambers of a transwell. Medium containing 100 ng/mL of recombinant mouse CXCL1 together with 0, 0.25, 1 or 4 µg/mL (5.7 mol/L ratio) of BHV1gG-Ig or 4 µg/mL of BAFF-R-Ig was placed in the lower chambers. Data represent the percentage of Gr1^{high}CD11b^{high} cells in the lower chamber divided by the total input of Gr1^{high}CD11b^{high} cells after 1 h of incubation at 37°C. (F) Mouse peritoneal cells (2×10^5) were placed in each of the upper chambers of a transwell. Medium containing 10 ng/mL of recombinant mouse CCL2 together with 0, 25, 100 or 400 ng/mL (5.7 mol/L ratio) of BHV1gG-Ig or 400 ng/mL of BAFF-R-Ig was placed in the lower chambers. Data represent the mean numbers of cells that attached to the membrane after 4 h of incubation at 37°C. * $P < 0.05$. Data are representative of three to four experiments.

vested at d 10 similarly showed more synovial hyperplasia and erosions in the controls than in the treated mice (data not shown). No neutrophils were detected in the synovium of control or treated mice either at d 10 or d 27, consistent with previous studies showing that neutrophil infiltration is an early feature of disease in the KRN model. Several genes linked to inflammation and cartilage/bone erosions such as *TNF α* , *IL-1 β* , *MMP-2* and *MMP-3* were upregulated in the joints of K/BxN serum-treated mice 5 d after arthritis induction. However, this upregulation was

not prevented by Ad-BHV1gG-Ig treatment (see Figure 4E).

Repeated Administration of BHV1gG-Ig Does Not Affect the Progression of Lupus Nephritis in NZB/W Mice

Given that BHV1gG binds to a number of chemokines that are upregulated in kidneys of NZB/W F1 mice at the early stages of lupus nephritis (9,15), we next tested whether BHV1gG-Ig treatment could alter the progression of renal disease in these mice. A 10-wk treatment with BHV1gG-Ig protein did not alter the onset of proteinuria or survival of 24-wk-

old NZB/W F1 mice (Figure 5A). One reason for this observation could be the development of an antibody response against the fusion protein. Indeed, IgG antibody against BHV1gG-Ig fusion protein started to appear in low titer in the serum of NZB/W F1 mice 2 wks after the first injection of BHV1gG-Ig and continued to increase for another 6 wks (data not shown). We therefore used the IFN α -accelerated lupus model which has shorter disease duration (22), to minimize the effects of an anti-BHV1gG-Ig humoral response. Twelve week-old NZB/W mice were injected IV with Ad-

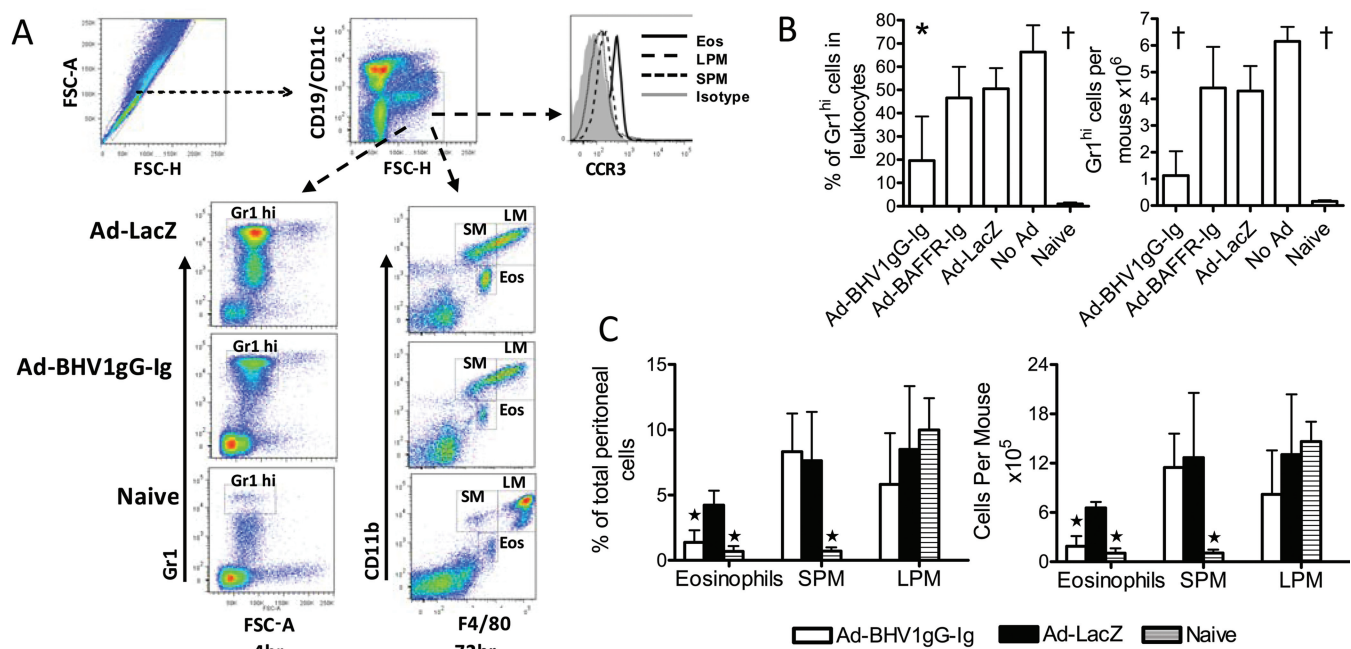


Figure 3. Treatment with Ad-BHV1gG-Ig significantly inhibits thioglycollate-induced neutrophil migration in BALB/c mice. Mice treated 4 d previously with Ad-BHV1gG-Ig or control adenovirus were injected IP with sterile thioglycollate. Mice were euthanized 4 or 72 h later and peritoneal cells were analyzed using flow cytometry. (A) Gating strategy and representative FACS plot of peritoneal cells from the mice. Gr1^{hi} cells (left) were identified as neutrophils whereas macrophages (right) are identified based on their expression of CD11b and F4/80. Eosinophils are CCR3+. (B) Percentages and numbers of Gr1^{hi} cells per peritoneal cavity of Ad-BHV1gG-Ig-treated (n = 5), control Ad-BAFFR-Ig (n = 5), control Ad-LacZ-treated (n = 5) or untreated mice (n = 4) 4 h after thioglycollate treatment. (C) Percentages and numbers of macrophages per peritoneal cavity of Ad-BHV1gG-Ig-treated, Ad-LacZ-treated or untreated mice 72 h after thioglycollate treatment (n = 4 for all groups). Horizontal lines denote the mean value for each group. The P values were compared with Ad-LacZ-treated mice. *P < 0.05, †P < 0.02. Data are representative of three experiments.

IFN α and were treated with BHV1gG-Ig from wk 13 to wk 21 or from wk 15 until the end of the experiment. The onset of proteinuria and survival were comparable between BHV1gG-Ig-treated mice (early treatment or late treatment) and untreated controls (Figure 5B). Examination of the kidneys from BHV1gG-Ig-treated mice revealed severe renal damage, macrophage infiltration and large lymphoid infiltrates, comparable with controls (data not shown).

DISCUSSION

Leukocyte infiltration is an important feature of the inflammatory response. Although a single chemokine may recruit more than one cell type, migration of multiple cell types in general requires a network of multiple chemokines and adhesion molecules. Some viruses manipulate the chemokine network by produc-

ing viral chemokine homologs, viral chemokine receptor homologs or viral chemokine binding proteins (26). The first identified herpesvirus-secreted chemokine-binding protein M3 interacts with multiple CC-, CXC-, CX3C-, and XC- chemokines at their receptor- and GAG-binding domains (26). Transgenic expression of M3 protein in pancreatic islets protects mice from streptozotocin-induced diabetes by inhibiting CCL2-mediated monocyte recruitment and CXCL13-induced B and T cell infiltration (27–28). BHV1gG-Ig binds to a broad range of chemokines, including many of those expressed in rheumatoid arthritis synovia and lupus kidneys (15), and, therefore, provides a convenient way of inhibiting multiple chemokines in autoimmune/inflammatory diseases. In this study, we asked whether this inhibitor could be delivered as a therapeutic agent

during the evolution of autoimmune disease *in vivo*. To accomplish this, we generated an adenovirus expressing BHV1gG-Ig fusion protein, allowing us to deliver a large quantity of BHV1gG-Ig *in vivo* in a rapid and convenient manner.

We show here that BHV1gG-Ig treatment successfully inhibited acute inflammation in two different animal models. Intraperitoneal injection of thioglycollate initiates an early influx of neutrophils followed by the later recruitment of eosinophils and monocytes/macrophages (20). Ad-BHV1gG-Ig treatment prevented the migration of both neutrophils and eosinophils but did not alter recruitment of inflammatory macrophages into the peritoneal cavity. Thioglycollate-induced neutrophil recruitment is mediated largely through the interaction of CXCR2 with its ligands CXCL1 and CXCL2 (29). We confirmed that BHV1gG inhibits neu-

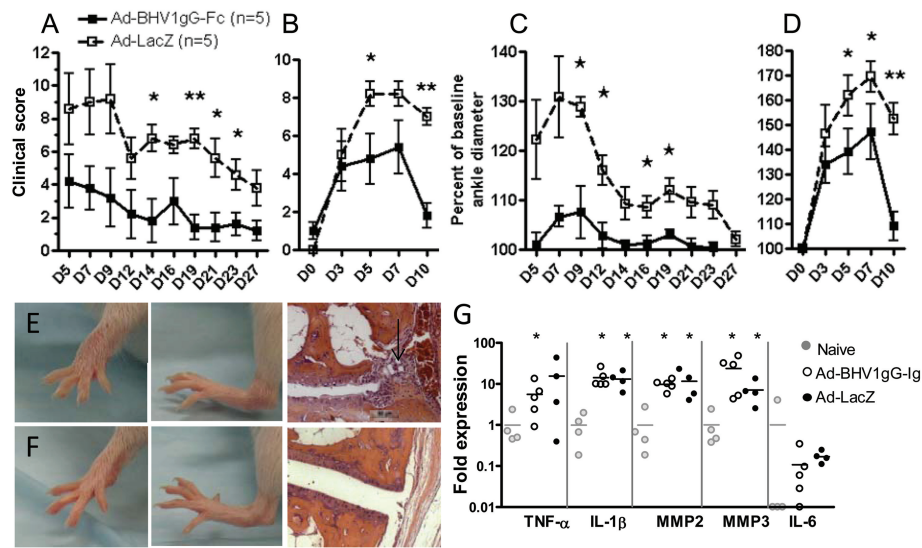


Figure 4. Administration of Ad-BHV1gG reduces the severity of K/BxN serum-induced arthritis in mice. (A) clinical scores of Ad-BHV1gG-Ig-treated or Ad-LacZ-treated mice with K/BxN serum-induced arthritis (Expt 1: average area under curve: Ad-BHV1gG-Ig-treated versus Ad-LacZ-treated = 49.9 ± 51.5 versus 142.8 ± 61.6 , mean \pm standard deviation; $P = 0.0317$). (B) clinical scores Expt 2. (C) average ankle diameters presented as percentage of baseline measurements of Ad-BHV1gG-Ig-treated or Ad-LacZ-treated mice with K/BxN serum-induced arthritis (Expt1: average area under curve: Ad-BHV1gG-Ig-treated versus Ad-LacZ-treated = 2286.6 ± 53.6 versus 2465.2 ± 121.4 , mean \pm standard deviation; $P = 0.0159$). (D) ankle diameters Expt 2. * $P < 0.05$, ** $P < 0.001$. (E, F) Representative pictures of front and hind paws of the mice from Expt 1 after at d 27 after the injection of K/BxN serum and treatment with either control Ad-LacZ (E) or Ad-BHV1gG-Ig (F). H and E staining of ankles shows joint space narrowing and inflammatory infiltrates in the Ad-LacZ-treated ankles but not in the ankles of Ad-BHV1gG-Ig-treated mice. Synovial hyperplasia scores (scored from 1 to 3) are 1.4 ± 1.4 in the controls and 0 ± 0 in the treated mice; $P = 0.04$. Bars in the histologic pictures represent 50 μ m. (G) Real-time PCR analysis of dissected synovium from naïve and K/BxN serum-induced mice at Day 5 * $P < 0.05$ compared with naïve controls.

trophil migration toward CXCL1 *in vitro*. Although BHV1gG does not bind to CXCL2, its interaction with CXCL1 (15) appears sufficient to prevent most of the peritoneal neutrophil accumulation. The small increase in peritoneal neutrophils observed in BHV1gG-treated mice might be due to the uninhibited chemoattractant activity of CXCL2, or to other unknown factors, given that inhibition of both CXCL1 and CXCL2 by monoclonal antibodies does not completely prevent thioglycollate-induced recruitment of neutrophils (29). It is not clear which chemokines drive the migration of eosinophils in thioglycollate-induced peritonitis model. However, CCR3 is expressed on the surface of the eosinophils

in the peritoneal cavity (Figure 3B) and it has been shown to mediate eosinophil recruitment in allergic disease (30). Given that CCL11, one of the ligands of CCR3, binds to BHV1gG (15), it is possible that BHV1gG inhibits thioglycollate-induced eosinophil migration through blocking the interaction of CCR3 with its ligands.

Monocyte recruitment in response to thioglycollate has been shown to depend largely on CCL2 and is independent of early neutrophil infiltration (31–32). Surprisingly, although BHV1gG binds to CCL2 *in vitro*, BHV1gG-Ig treatment did not impair thioglycollate-induced monocyte accumulation *in vivo* (15). This may reflect a redundant role of other

chemokines such as CCL6 in thioglycollate-induced monocyte migration (33). Alternatively, BHV1gG may bind to CCL2 with low affinity or at a site that is not essential to its interaction with its receptor CCR2. It is also possible that Ad-BHV1gG-Ig treatment could influence the number of circulating monocytes as it also binds to CXCL12, a key chemokine for bone marrow sequestration of monocytes. A failure of CXCL12-mediated sequestration in the bone marrow may offset any inhibitory effects of BHV1gG on CCL2-dependent monocyte trafficking into the peritoneal cavity (34). Further studies will be needed to discriminate between these hypotheses. In summary, our study demonstrated that BHV1gG is capable of inhibiting the migration of polymorphonuclear cells, but not macrophages, into the inflamed peritoneum.

In accordance with this result, Ad-BHV1gG-Ig treatment significantly reduced joint inflammation in the K/BxN serum transfer arthritis model. Arthritis in this model is initiated by the binding of autoantibody contained in K/BxN serum to its target glucose-6-phosphate isomerase (GPI) in the recipient mice (25). The immune complex then activates circulating neutrophils and synovial mast cells through Fc γ RIII, leading to degranulation of these cells and increased vascular permeability. As a result, autoantibodies are able to enter synovial space in large quantities and bind to GPI expressed on bone surfaces. This leads to synovial inflammation characterized by activation of the complement system, recruitment and activation of neutrophils, activation of resident synovial cells such as mast cells, macrophages and fibroblasts, as well as production of inflammatory cytokines such as TNF α and IL-1 β . CXCL1, CXCL2 and CXCL5 all are upregulated in the synovial tissues of K/BxN serum-treated mice (2,35). Consistent with this observation, CXCR2-mediated neutrophil recruitment has been shown to be critical for the induction of arthritis in this model (35). Targeting CXCL1 with a monoclonal antibody has, however,

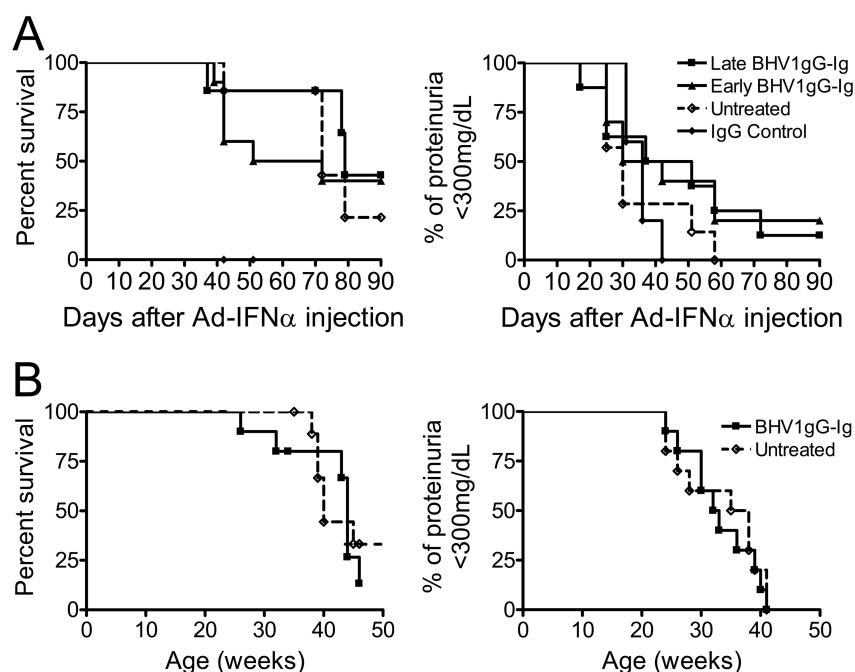


Figure 5. Repeated administration of BHV1gG protein does not alter the progression of lupus in NZB/W F1 mice with or without previous treatment with Ad-IFN α . (A) NZB/W F1 mice were injected IV with Ad-IFN α at 12 wks of age and were treated with 500 μ g of BHV1gG-Ig three times a week from wk 13 to 21 (early BHV1gG-Ig) or from wk 15 until the end of the experiment (late BHV1gG-Ig). (B) Twenty-four-week-old NZB/W F1 mice were treated with 500 μ g of BHV1gG-Ig three times a week until 34 wks of age. Survival (left) and age at proteinuria onset (right) of the mice are shown.

shown only modest inhibitory effects on the clinical index of K/BxN serum-induced arthritis (18). CXCL1 is one of the chemokines that BHV1gG can bind with high affinity (15) and, as shown here, the fusion protein inhibits CXCL1-mediated neutrophil migration *in vitro*. It is plausible, however, given the failure of CXCL1 targeting alone to prevent arthritis induced by high dose K/BxN serum transfer (18), that Ad-BHV1gG-Ig treatment protects mice from K/BxN-induced arthritis at least in part through interrupting other chemokine–chemokine receptor interactions in addition to that of CXCL1 with CXCR2. Despite significantly reducing arthritis severity, BHV1gG-Ig treatment did not affect local expression of a number of inflammatory mediators including *IL-1 β* , *TNF α* , *MMP-2* or *MMP-3*. *IL-1 β* and *TNF α* are essential for the initiation of arthritis in this model; these cytokines can be pro-

duced by local mast cells (36). In fact, it has been shown that neutrophil-derived *TNF α* is completely dispensable in this model, whereas neutrophil-derived *IL-1 β* contributes only modestly to the synovial inflammation (37). In addition, synovial fibroblasts have been shown to be capable of producing *IL-1 β* , *MMP-2* and *MMP-3* *in vitro* (35). Thus BHV1gG inhibits polymorphonuclear cell migration into the joint at a stage downstream of the initial local inflammatory response.

Although antagonists of CCR1, CCR2 or CCR5 all reduce the severity of arthritis in animal models (38–40), CCR2 and CCR5 antagonists failed to show additional benefit over standard therapy in clinical trials for rheumatoid arthritis (7,41–44), and a recent phase II clinical trial of a CCR1 antagonist reported only modest results (45). These studies show that single chemokine blockade is unlikely to have sufficient therapeutic effi-

cacy in patients with rheumatoid arthritis and suggest that evaluation of multiple chemokine blockade may be warranted (46–47).

We also wished to test whether BHV1gG-Ig treatment affects a model of chronic inflammation in which neutrophils do not participate. We chose to use NZB/W F1 mice which spontaneously develop chronic nephritis characterized by infiltration of T and B lymphocytes, macrophages and dendritic cells with almost no neutrophil involvement (48–50). Studies that genetically target chemokine or chemokine receptors in lupus-prone mice have begun to reveal the mechanism by which chemokines direct leukocyte trafficking in lupus nephritis. Deficiency of *CCL2* or *CCR2* reduces interstitial and glomerular infiltration of macrophages and protects MRL/lpr mice from lupus nephritis (5–6). In contrast, *CXCR3* deficiency only decreases interstitial but not glomerular macrophage infiltration in MRL/lpr mice (12). These mice also have less renal infiltration of inflammatory T cells and a milder nephritis compared with the wild type controls. Interestingly, *CXCR3* deficiency does not protect NZB/W F1 mice from lupus nephritis, indicating that the role of *CXCR3* in kidney inflammation varies in mice of different genetic backgrounds (51). Finally, deficiency of *CCR5*, which shares two ligands (*CCL3* and *CCL5*) with *CCR1*, is also protective in MRL/lpr mice (52). These studies have mostly highlighted the distinct role of individual chemokine receptors in lupus nephritis.

A number of chemokines and chemokine receptors have been targeted with biologic antagonists in animal models of lupus. In accordance with the genetic data, treatment with a *CCL2* antagonist reduces nephritis activity in MRL/lpr mice and lowers the dose of cyclophosphamide required to abrogate disease (53). Treatment with a *CX3CR1* antagonist similarly inhibits both glomerular and interstitial leukocyte infiltration, and reduces glomerular pathology in MRL/lpr mice (14). Fur-

thermore, treatment with a CCR1 antagonist can reduce interstitial but not glomerular infiltration of macrophages in MRL/lpr mice with established nephritis and improve kidney function of these mice without reversing glomerular injury (13). Taken together, these studies have begun to reveal the complex nature of the chemokine network in lupus nephritis. It remains a great challenge to target chemokines in lupus nephritis as the distinct role of each chemokine and the impact of strain differences need to be further elucidated.

Among the chemokines that are upregulated in the kidneys of NZB/W F1 mice before or upon the onset of proteinuria (9), CXCL13, CCL2, CCL3, CCL5 and CCL20 all can bind BHV1gG *in vitro* (15). Despite its binding to multiple chemokines that are upregulated early in the progress of nephritis in NZB/W F1 mice and its inhibition of the biological functions of at least one of these chemokines, CXCL13, treatment with BHV1gG-Ig failed to affect either the onset of proteinuria, renal macrophage infiltration, accumulation of lymphoid aggregates or the survival of NZB/W F1 mice. In addition, BHV1gG-Ig treatment did not affect the progression of disease in IFN α -treated NZB/W F1 mice which develop an accelerated disease characterized by high expression of CXCL13 and macrophage infiltration (9). The lack of effect of BHV1gG-Ig treatment on NZB/W F1 mice is consistent with its lack of effect on macrophage infiltration in the thioglycollate peritonitis model and its lack of inhibition of CCL2-mediated migration *in vitro*. It remains possible, however, given the inflammatory state of the mice, that we were unable to achieve a sufficient serum concentration of BHV1gG to achieve inhibition of the relevant chemokines.

CONCLUSION

Our results suggest that BHV1gG-Ig is capable of inhibiting CXC chemokine-induced cell signaling and migration *in vivo* and clearly prevents the initiation of acute inflammation by inhibiting infiltra-

tion of neutrophils and eosinophils into inflammatory sites. This demonstrates the potential of a multi-chemokine inhibitor strategy in treating acute inflammatory diseases. In contrast, BHV1gG-Ig does not have a therapeutic effect in a disease characterized by macrophage and lymphoid cell driven inflammation. Given its viral origin, it is not surprising that repeated administration of BHV1gG-Ig induces an antibody response against this protein. A better understanding of the molecular mechanism of its binding to multiple structurally different chemokines may allow the design of a small molecule which retains the inhibitory efficacy of BHV1gG-Ig without its immunogenicity.

ACKNOWLEDGMENTS

This work was supported by NIDDK R01 DK085241-01 and Rheuminations.

DISCLOSURE

The authors declare that they have no competing interests as defined by *Molecular Medicine*, or other interests that might be perceived to influence the results and discussion reported in this paper.

REFERENCES

- Iwamoto T, Okamoto H, Toyama Y, Momohara S. (2008) Molecular aspects of rheumatoid arthritis: chemokines in the joints of patients. *FEBS J.* 275:4448–55.
- Jacobs JP, et al. (2010) Deficiency of CXCR2, but not other chemokine receptors, attenuates autoantibody-mediated arthritis in a murine model. *Arthritis Rheum.* 62:1921–32.
- Laragione T, Brenner M, Sherry B, Gulko PS. (2011) CXCL10 and its receptor CXCR3 regulate synovial fibroblast invasion in rheumatoid arthritis. *Arthritis Rheum.* 63:3274–83.
- Zheng B, et al. (2005) CXCL13 neutralization reduces the severity of collagen-induced arthritis. *Arthritis Rheum.* 52:620–6.
- Yellin M, et al. (2012) A phase II, randomized, double-blind, placebo-controlled study evaluating the efficacy and safety of MDX-1100, a fully human anti-CXCL10 monoclonal antibody, in combination with methotrexate in patients with rheumatoid arthritis. *Arthritis Rheum.* 64:1730–9.
- Takeuchi T, Kameda H. (2012) What is the future of CCR5 antagonists in rheumatoid arthritis? *Arthritis Res. Ther.* 14:114.
- Vergunst CE, et al. (2008) Modulation of CCR2 in rheumatoid arthritis: a double-blind, random-

- ized, placebo-controlled clinical trial. *Arthritis Rheum.* 58:1931–9.
- Lebre MC, et al. (2011) Why CCR2 and CCR5 blockade failed and why CCR1 blockade might still be effective in the treatment of rheumatoid arthritis. *PLoS One.* 6:e21772.
- Schiffer L, et al. (2008) Activated renal macrophages are markers of disease onset and disease remission in lupus nephritis. *J. Immunol.* 180:1938–47.
- Perez de Lema G, et al. (2005) Chemokine receptor Ccr2 deficiency reduces renal disease and prolongs survival in MRL/lpr lupus-prone mice. *J. Am. Soc. Nephrol.* 16:3592–601.
- Tesch GH, Maifert S, Schwarting A, Rollins BJ, Kelley VR. (1999) Monocyte chemoattractant protein 1-dependent leukocytic infiltrates are responsible for autoimmune disease in MRL-Fas(lpr) mice. *J. Exp. Med.* 190:1813–24.
- Steinmetz OM, et al. (2009) CXCR3 mediates renal Th1 and Th17 immune response in murine lupus nephritis. *J. Immunol.* 183:4693–704.
- Anders HJ, et al. (2004) Late onset of treatment with a chemokine receptor CCR1 antagonist prevents progression of lupus nephritis in MRL-Fas(lpr) mice. *J. Am. Soc. Nephrol.* 15:1504–13.
- Inoue A, et al. (2005) Antagonist of fractalkine (CX3CL1) delays the initiation and ameliorates the progression of lupus nephritis in MRL/lpr mice. *Arthritis Rheum.* 52:1522–33.
- Bryant NA, Davis-Poynter N, Vanderplasschen A, Alcamí A. (2003) Glycoprotein G isoforms from some alphaherpesviruses function as broad-spectrum chemokine binding proteins. *EMBO J.* 22:833–46.
- Ramanujam M, et al. (2004) Mechanism of action of transmembrane activator and calcium modulator ligand interactor-Ig in murine systemic lupus erythematosus. *J. Immunol.* 173:3524–34.
- Mihara M, et al. (2000) CTLA4Ig inhibits T cell-dependent B-cell maturation in murine systemic lupus erythematosus. *J. Clin. Invest.* 106:91–101.
- Santos LL, et al. (2011) Macrophage migration inhibitory factor regulates neutrophil chemotactic responses in inflammatory arthritis in mice. *Arthritis Rheum.* 63:960–70.
- Wiese K, et al. (2012) Defective macrophage migration in Galphai2- but not Galphai3-deficient mice. *J. Immunol.* 189:980–7.
- Ghosn EE, et al. (2010) Two physically, functionally, and developmentally distinct peritoneal macrophage subsets. *Proc. Natl. Acad. Sci. U. S. A.* 107:2568–73.
- Jirholt J, et al. (1998) Genetic linkage analysis of collagen-induced arthritis in the mouse. *Eur. J. Immunol.* 28:3321–8.
- Liu Z, et al. (2011) Interferon-alpha accelerates murine systemic lupus erythematosus in a T cell-dependent manner. *Arthritis Rheum.* 63:219–29.
- Shi K, et al. (2001) Lymphoid chemokine B cell-attracting chemokine-1 (CXCL13) is expressed in germinal center of ectopic lymphoid follicles within the synovium of chronic arthritis patients. *J. Immunol.* 166:650–5.

24. Soto H, *et al.* (2008) Gene array analysis comparison between rat collagen-induced arthritis and human rheumatoid arthritis. *Scand J. Immunol.* 68:43–57.
25. Kyburz D, Corr M. (2003) The KRN mouse model of inflammatory arthritis. *Springer Semin. Immunopathol.* 25:79–90.
26. Alcamí A. (2003) Viral mimicry of cytokines, chemokines and their receptors. *Nat. Rev.* 3:36–50.
27. Martin AP, Canasto-Chibuque C, Shang L, Rollins BJ, Lira SA. (2006) The chemokine decoy receptor M3 blocks CC chemokine ligand 2 and CXC chemokine ligand 13 function in vivo. *J. Immunol.* 177:7296–302.
28. Martin AP, *et al.* (2007) The chemokine binding protein M3 prevents diabetes induced by multiple low doses of streptozotocin. *J. Immunol.* 178:4623–31.
29. Wengner AM, Pitchford SC, Furze RC, Rankin SM. (2008) The coordinated action of G-CSF and ELR + CXC chemokines in neutrophil mobilization during acute inflammation. *Blood.* 111:42–9.
30. Wegmann M. (2011) Targeting eosinophil biology in asthma therapy. *Am. J. Respir. Cell Mol. Biol.* 45:667–74.
31. Henderson RB, Hobbs JA, Mathies M, Hogg N. (2003) Rapid recruitment of inflammatory monocytes is independent of neutrophil migration. *Blood.* 102:328–35.
32. Takahashi M, Galligan C, Tessarollo L, Yoshimura T. (2009) Monocyte chemoattractant protein-1 (MCP-1), not MCP-3, is the primary chemokine required for monocyte recruitment in mouse peritonitis induced with thioglycollate or zymosan A. *J. Immunol.* 183:3463–71.
33. LaFleur AM, Lukacs NW, Kunkel SL, Matsukawa A. (2004) Role of CC chemokine CCL6/C10 as a monocyte chemoattractant in a murine acute peritonitis. *Mediators Inflamm.* 13:349–55.
34. Wang Y, *et al.* (2009) CCR2 and CXCR4 regulate peripheral blood monocyte pharmacodynamics and link to efficacy in experimental autoimmune encephalomyelitis. *J. Inflamm. (Lond.).* 6:32.
35. Sadik CD, Kim ND, Alekseeva E, Luster AD. (2011) IL-17RA signaling amplifies antibody-induced arthritis. *PLoS One.* 6:e26342.
36. Ji H, *et al.* (2002) Critical roles for interleukin 1 and tumor necrosis factor alpha in antibody-induced arthritis. *J. Exp. Med.* 196:77–85.
37. Monach PA, *et al.* (2010) Neutrophils in a mouse model of autoantibody-mediated arthritis: critical producers of Fc receptor gamma, the receptor for C5a, and lymphocyte function-associated antigen 1. *Arthritis Rheum.* 62:753–64.
38. Plater-Zyberk C, Hoogewerf AJ, Proudfoot AE, Power CA, Wells TN. (1997) Effect of a CC chemokine receptor antagonist on collagen induced arthritis in DBA/1 mice. *Immunol. Lett.* 57:117–20.
39. Quinones MP, *et al.* (2005) The complex role of the chemokine receptor CCR2 in collagen-induced arthritis: implications for therapeutic targeting of CCR2 in rheumatoid arthritis. *J. Mol. Med. (Berl.).* 83:672–81.
40. Vierboom MP, *et al.* (2005) Inhibition of the development of collagen-induced arthritis in rhesus monkeys by a small molecular weight antagonist of CCR5. *Arthritis Rheum.* 52:627–36.
41. Fleishaker DL, *et al.* (2012) Maraviroc, a chemokine receptor-5 antagonist, fails to demonstrate efficacy in the treatment of patients with rheumatoid arthritis in a randomized, double-blind placebo-controlled trial. *Arthritis Res. Ther.* 14: R11.
42. Gerlag DM, *et al.* (2010) Preclinical and clinical investigation of a CCR5 antagonist, AZD5672, in patients with rheumatoid arthritis receiving methotrexate. *Arthritis Rheum.* 62:3154–60.
43. van Kuijk AW, *et al.* (2010) CCR5 blockade in rheumatoid arthritis: a randomised, double-blind, placebo-controlled clinical trial. *Ann. Rheum. Dis.* 69:2013–6.
44. Vergunst CE, *et al.* (2009) MLN3897 plus methotrexate in patients with rheumatoid arthritis: safety, efficacy, pharmacokinetics, and pharmacodynamics of an oral CCR1 antagonist in a phase IIa, double-blind, placebo-controlled, randomized, proof-of-concept study. *Arthritis Rheum.* 60:3572–81.
45. Tak PP, *et al.* (2012) Chemokine receptor CCR1 antagonist CCX354-C treatment for rheumatoid arthritis: CARAT-2, a randomised, placebo controlled clinical trial. *Ann. Rheum. Dis.* 72:337–44.
46. Szekanecz Z, Koch AE, Tak PP. (2011) Chemokine and chemokine receptor blockade in arthritis, a prototype of immune-mediated inflammatory diseases. *Neth. J. Med.* 69:356–66.
47. Zhao Q. (2010) Dual targeting of CCR2 and CCR5: therapeutic potential for immunologic and cardiovascular diseases. *J. Leukoc. Biol.* 88:41–55.
48. Cassese G, *et al.* (2001) Inflamed kidneys of NZB/W mice are a major site for the homeostasis of plasma cells. *Eur. J. Immunol.* 31:2726–32.
49. Liu Z, *et al.* Interferon alpha accelerates murine SLE in a T cell dependent manner. *Arthritis Rheum.* 63:219–29.
50. Schiffer L, *et al.* (2003) Short term administration of costimulatory blockade and cyclophosphamide induces remission of systemic lupus erythematosus nephritis in NZB/W F1 mice by a mechanism downstream of renal immune complex deposition. *J. Immunol.* 171:489–97.
51. Moser K, *et al.* (2012) CXCR3 promotes the production of IgG1 autoantibodies but is not essential for the development of lupus nephritis in NZB/NZW mice. *Arthritis Rheum.* 64:1237–46.
52. Turner JE, *et al.* (2012) Protective role for CCR5 in murine lupus nephritis. *Am. J. Physiol. Renal Physiol* 302: F1503–15.
53. Kulkarni O, *et al.* (2009) Anti-Ccl2 Spiegelmer permits 75% dose reduction of cyclophosphamide to control diffuse proliferative lupus nephritis and pneumonitis in MRL-Fas(lpr) mice. *J. Pharmacol. Exp. Ther.* 328:371–7.